FERMILAB-PUB-17-051-PPD
(accepted)

Thermal conductance characterization of a pressed copper rope strap between 0.13 K and 10 K

R. C. Dhuley[1], M. Ruschman[1], J. T. Link[2], and J. Eyre[2]

[1]Fermi National Accelerator Laboratory, Batavia, IL 60510, United States
[2]Technology Applications, Inc. (TAI), Boulder, CO 80301, United States

Abstract

Mechanically pressing the ends of a copper braid in solid copper is an effective way of constructing solderless conductive straps for cryogenic applications. In this paper we present thermal conductance data of such a copper strap measured using the two-heater one-thermometer method. The measurements span a wide temperature range of 0.13 K – 10 K applicable to a variety of cryogenic systems employing liquid helium, pulse tube coolers, adiabatic demagnetization refrigerators, and others. Above ≈1.5 K, the braid thermal conductivity dominates the strap conductance resulting in a near-linear dependence with temperature. The variation with temperature below ≈1.5 K is near-quadratic indicating dominance of the pressed contact conductance at the strap ends. Electron-beam welding the braid to the strap ends is shown to be a promising solution for improving sub-Kelvin thermal conductance of the strap.

1. Introduction

Flexible thermal linkages have been used vitally by several cryogenic systems, for example [**1-4**], to meet their requirements of high thermal conductance between components while accommodating movements due to thermal contractions and isolating mechanical vibrations. For the same purpose the cryostat of SuperCDMS-SNOLAB, a proposed dark matter search experiment, will use flexible straps on its 4.5 K, 1 K, 250 mK, and 15 mK thermal stages. While two candidate materials viz. copper [**5**] and aluminum [**6**] may be engineered into straps for low temperatures, stringent radio-purity requirements of the experiment limit to strictly using copper for the straps. Solderless straps constructed by mechanically pressing the ends of a copper braid in solid blocks of copper are an attractive option for the SuperCDMS-SNOLAB cryostat.

In this paper we present thermal conductance measurements on a candidate strap in the 0.13 K – 1 K temperature range and characterize the observed trends in the conductance based on the physical mechanisms of heat transfer through the strap. We further explore, via literature study and experiments, potential methods such as annealing and electron-beam welding for improving the strap conductance.

2. Strap details

The strap under investigation is a Technology Applications, Inc. (TAI) Copper Thermal Strap (CuTS™) Model P5-502. The braid (cabling of fine copper strands) is cold-pressed at each of its ends in slotted copper blocks (end-lugs). The pressing operation is carried out in open

This manuscript has been authored by Fermi Research Alliance, LLC under Contract No. DE-AC02-07CH11359 with the U.S. Department of Energy, Office of Science, Office of High Energy Physics. The U.S. Government retains and the publisher, by accepting the article for publication, acknowledges that the U.S. Government retains a non-exclusive, paid-up, irrevocable, world-wide license to publish or reproduce the published form of this manuscript, or allow others to do so, for U.S. Government purposes.

atmosphere by means of a mechanical press. Both the braid and end-lugs are 99.98% pure OFHC copper. The strap is shown in **figure 1** and its dimensions are listed in **Table 1**.

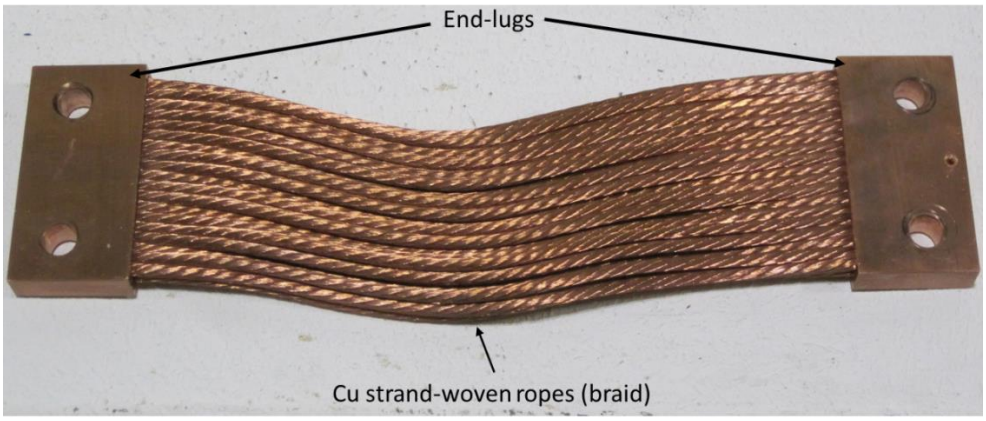

Figure 1: Photograph of a TAI's Copper Thermal Strap (CuTS™) Model P5-502 strap displaying the copper strand-woven rope braid and the end-lugs.

Table 1: Dimensional parameters of the tested TAI's Copper Thermal Straps (CuTS™) Model P5-502

Dimension	Value
Rope cross section, A	5E-6 m^2
Rope porosity, p	0.645
# ropes, n	36
Braid/cabling length, L	0.15 m, 0.1 m*

*The 0.1 m long strap was used in developmental e-beam welding (see Section 5b)

3. Measurement apparatus and procedure

a) Apparatus and instrumentation

The strap thermal conductance was measured between 4 K and 10 K on a pulse tube refrigerator (PT) and on an adiabatic demagnetization refrigerator (ADR) in the 0.13 K - 3 K range. **Figure 2** shows a schematic of the measurement setup. One end-lug of the strap was bolted to the refrigerator cold plate (CP). We will hereafter refer this end-lug as 'cold end-lug' while the other end-lug will be termed as 'warm end-lug'. The warm end-lug hung off the cold end-lug via two kevlar threads (length 5", diameter 0.04"). The heaters, Q_H and Q_C were thermally bonded respectively to the warm and cold end-lugs. Another heater Q_{CP} attached to the PT cold plate controlled the base temperature of the assembly, while salt pill magnetization provided this control on the ADR. The thermometer, T_H measured the warm end-lug temperature and the thermometer, T_{CP} monitored the cold plate temperature and its stability. **Table 2** lists details of the instrumentation used to obtain the strap thermal conductance.

Table 2: Details of the instrumentation used for strap conductance measurement

Element	PT test (4 K - 10 K)	ADR test (0.13 K - 3 K)
T_H	Lakeshore Cernox	Lakeshore RuO**,** Lakeshore Cernox
T_{CP}	Scientific Instruments Si diode	Scientific Instruments RuO
Q_H, Q_C, Q_{CP}	Minco Polymide Thermofoil	Metal Film resistor

b) Measurement procedure

We obtained thermal conductance of the strap following the two-heater one-thermometer method of thermal conductance measurement **[7]**:

1. With the assembly at the refrigerator no-load temperature, Q_H was powered to a value ` Q '. The heater Q_C was not powered in the step. Temperature ' T_1 ' at T_H was noted after the assembly attained a steady state.

2. Q_H was then switched off and Q_C was powered to within 0.2% of Q . After the assembly attained a steady state, temperature ` T_2 ' at T_H was noted. Q_C was then switched off.

3. Between steps 1 and 2, T_{CP} indicated (and ensured) that the cold plate temperature was unchanged within 5 mK for the PT and within 0.5 mK for the ADR measurements. Strap thermal conductance, K_{strap} was then calculated as:

$$K_{strap}(T_{base}) = \frac{Q}{T_1 - T_2}, \tag{1}$$

where $T_{base} = 0.5(T_1 + T_2)$ is the base temperature.

4. The assembly was heated from no-load temperature to several higher base temperatures in steps by incrementing the power into Q_{CP} (on the PT) or by magnetization (on the ADR). At each base temperature, strap conductance was obtained following steps 1-3. The temperature difference $T_1 - T_2$ was typically 2% of the T_{base} .

c) Measurement uncertainty and stray heat leak

The following uncertainties hold for our measurements: heater voltage- 0.004%, heater resistance- 1%, and temperature difference- 2 mK on the PT and 0.2 mK on the ADR (instrument resolution). The largest contributor to the conductance uncertainty is the uncertainty in the temperature difference (<8%).

The stray heat leak from the three sources- Kevlar thread suspension, electrical lead wires of the thermometers and heaters, and the enclosure radiation is less than 0.25% and 0.1% of the smallest heater power input during the PT and ADR measurements respectively.

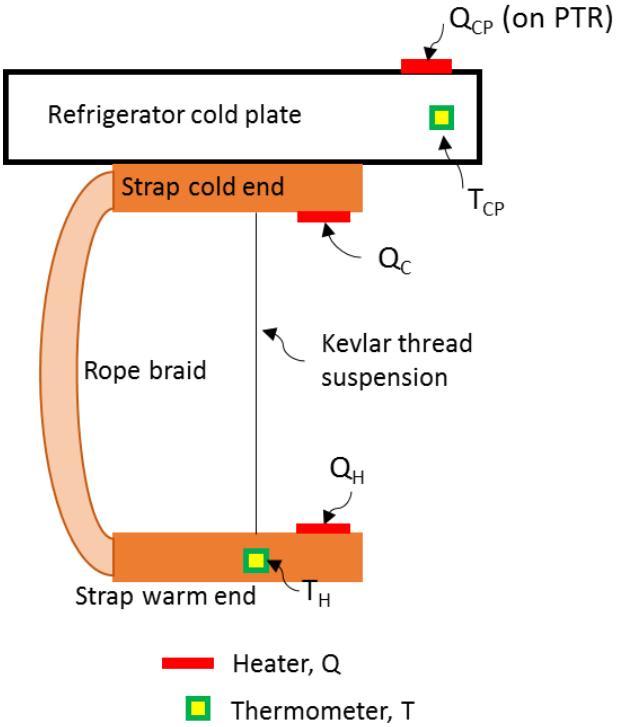

Figure 2: Schematic of the thermal conductance measurement setup highlighting instrumentation for the two-heater one-thermometer method.

4. Results: Strap conductance

Figure 3 shows the strap conductance in the 0.13 K – 10 K temperature range plotted on a log-log scale along with the measurement uncertainty. The error bars are not distinctly visible on the graph due to the log-log scale. The PT data and the ADR data respectively carry maximum uncertainties of 3% and 9%. Starting at 10 K the strap conductance initially falls gradually with temperature down till ≈1.5 K. At ≈1.5 K, the conductance starts to fall steeper and continues at this rate down to the lower end of measurements (0.13 K). We fit the data with power laws using the least squares method. **Figure 3** shows that two distinct power laws fit the data depending on the temperature range- a near-quadratic power law below 1.5 K and a near-linear power law above 1.5 K. **Table 3** lists the fitting coefficients with their standard errors as well as goodness of fits.

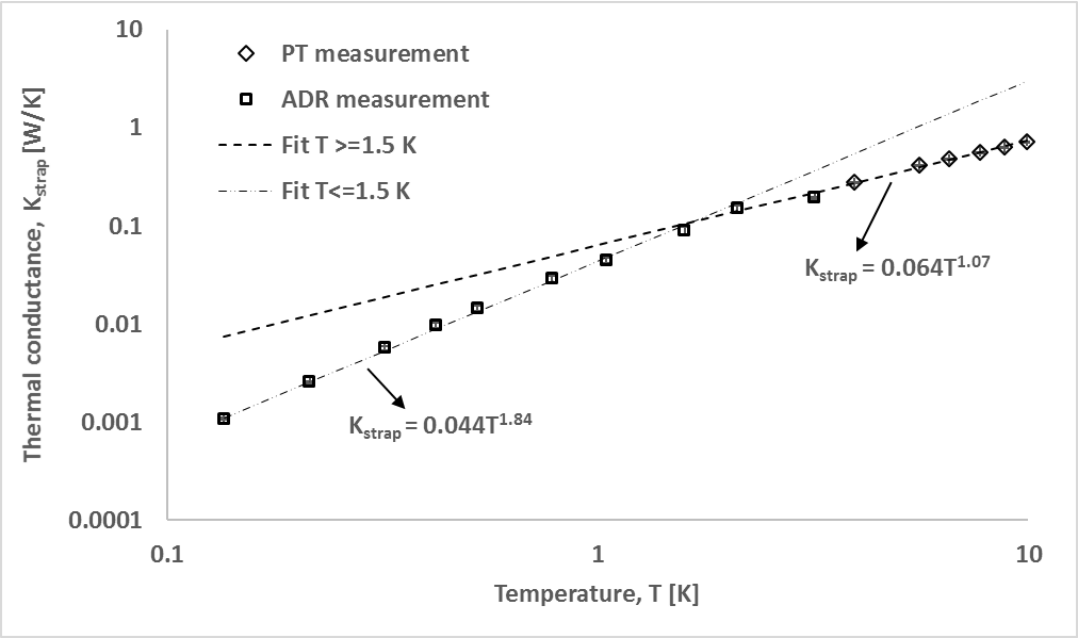

Figure 3: Strap thermal conductance as a function of temperature in the 0.13 K – 10 K range. Also plotted are the two power law fits that follow the data above and below 1.5 K. Both fit lines are extrapolated over the entire range of measurements for visual clarity.

Table 3: Details of the power law fits to the strap thermal conductance vs. temperature data

Fit temperature range	Coefficients 'a' and 'b' in $K_{strap}[W/K] = aT^b$		Goodness of fit, R^2
	a	b	
0.13 K – 1.5 K	0.044 ± 0.002	1.84 ± 0.03	0.9933
1.5 K – 10 K	0.064 ± 0.004	1.07 ± 0.03	0.9936

5. Analysis and discussion

a) The two power laws

Two different dependencies of the strap conductance on temperature in the two temperature ranges point to two different physical mechanisms by which the strap conducts heat. Based on the strap construction, we can write the strap conductance, K_{strap} as a series sum of its constituent conductances:

$$\frac{1}{K_{strap}} = \frac{1}{K_{braid}} + \frac{1}{K_{pressed}}, \tag{2}$$

where K_{braid} is the braid conductance and $K_{pressed}$ is the combined conductance at the two pressed ends. The braid conductance is simply the conductance of the copper strand-woven ropes and can be modeled as $K_{braid} = Gk_{Cu}(T)$, where $G(= pnA/L)$ is the geometric factor and $k_{Cu}(T)$

is the temperature dependent thermal conductivity of copper. In the temperature range of interest, OFHC copper exhibits predominantly electronic conduction so that the conductivity will vary linearly with temperature as $k_{Cu}(T) = \alpha T$. The parameter α depends on the copper purity and can be determined from the residual resistance ratio (RRR) of the braid copper. On the other hand, $K_{pressed}$ is the contact conductance between the ends of the braid and the strap end-lug.

Cryogenic heat conduction across pressed metallic contacts has been extensively studied in the literature [**8-10**]. Although under varying experimental conditions and the findings being largely empirical in nature, the investigations bring out certain common characteristics of pressed contact conductance. First, the conductance is independent of the macroscopic or apparent contact area [**8**] as the heat is carried across the joint through the contacting microscopic asperities. Second, near liquid helium temperatures the conductance follows a power law with temperature with the exponent between one and three [**11**]. The exponent is nearly unity for clean surfaces where there is pure metal-metal contact giving way to electronic conduction. If the surfaces are coated with an insulating material such as an oxide layer, where electronic conduction may exist poorly, heat is carried across the contact by phonons. Pure phonon heat transfer across contacts exhibits a cubic power law with temperature. For contacts between flat copper surfaces, which typically carry a native oxide layer [**12**] formed during handling, several experiments have shown the contact conductance to vary as nearly temperature-squared [**11,13,14**]. In the following, we find that even pressed joints between strand-woven copper braid (porous ropes) and solid copper, in the presence of copper oxide, exhibit conductance varying nearly as temperature squared.

We obtained the rope RRR by measuring electrical resistance of the strap rope sample at room temperature of 293 K and then near 4 K on the pulse tube refrigerator. The RRR measurement apparatus is schematically shown in **figure 4**. A 44" rope sample was wound as a helix along a thin kapton tape plated copper sheet roll. The kapton tape electrically isolated the rope from the copper roll. The roll was affixed to the PT cold plate using a hose clamp. Resistance was measured using the DC four-wire method. As illustrated in **figure 4**, voltage taps were kept `inside' of the current taps for removing any lead wire-rope contact resistance that would otherwise appear in the voltage measurement loop. The measurement gave RRR of 77 ± 1. Values of α as a function of RRR were obtained using NIST empirical functions for OFHC copper thermal conductivity [**15**]. **Figure 5** shows α corresponding to the RRR values of 50, 100, and 150 and the interpolation used to obtain α at RRR = 77. The calculated value is α = 117 W/m-K^2. Using the braid geometric factor G = 0.000785 m, the braid conductance is $K_{braid}(T) = 0.092T[K]$ in the unit of W/K. With $K_{strap}(T)$ and $K_{braid}(T)$ known, we obtain $K_{pressed}$ from **eq (2)**.

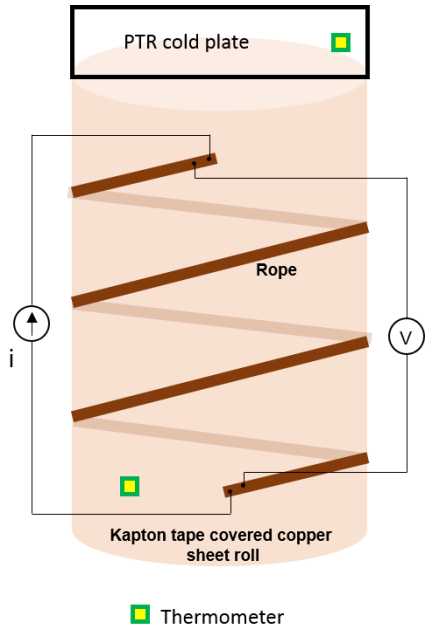

Figure 4: Schematic of the rope RRR measurement setup showing the DC 4-wire method.

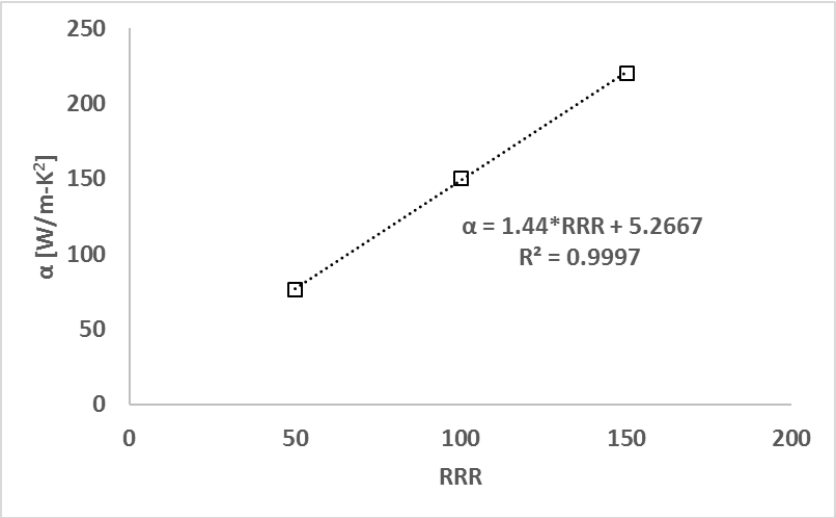

Figure 5: The parameter α as a function of copper RRR obtained from the NIST data for OFHC copper thermal conductivity [**15**]. The NIST OFHC conductivity obeys $k_{Cu}(T) = \alpha T$ at least up to 10 K for all the stated RRRs.

Figure 6 plots and compares K_{strap}, K_{braid}, and $K_{pressed}$. A least squares fit to the $K_{pressed}$ vs. temperature data gives a power law $K_{pressed}[W/K] = 0.07T^{1.91}$ in the temperature range of 0.13 K - 10 K with R^2 goodness of fit of 0.9875. This conductance-temperature behavior is very well consistent with flat contacts of oxidized copper surfaces [**11**]. This similarity among a contact

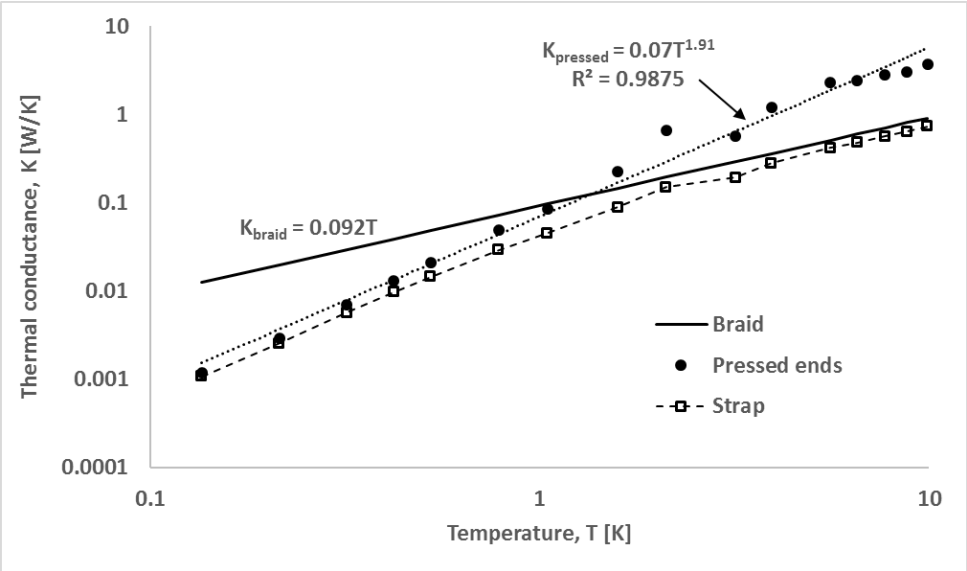

Figure 6: Strap thermal conductance separated out two into braid conductance, K_{braid} and the pressed ends conductance, $K_{pressed}$. K_{braid} is a linear function of temperature derived from the measured rope RRR. $K_{pressed}$ is fitted using least squares method and is seen to follow a near-quadratic power law. The dash-line through K_{strap} is a guide to the eye. The data are for the 150 mm long strap.

between two flat surfaces and that between strand-woven ropes with a flat surface can be partly justified using the fact that the contact conductance is independent of the apparent surface area. It can be argued that for a given apparent contact area, a joint between strand-woven ropes and a flat surface may have microscopic contact area (through which the heat actually transfers) comparable to that between two flat surfaces. Additionally, while the ropes are being pressed during strap assembly, exposure to atmospheric air will likely form oxide on surfaces [**12**] of the rope strands and the end-lugs. The pressed joint components therefore will carry a native copper oxide layer so that the heat transfer will be via the same physical mechanisms as those between two oxidized flat copper surfaces.

The near-quadratic dependence of $K_{pressed}$ and the linear dependence of K_{braid} on temperature immediately explain the behavior of K_{strap} seen in **figure 3**. The near-linear variation in K_{strap} above ≈1.5 K arises because K_{strap} in this range is dominated by K_{braid} while the near-quadratic variation comes from the dominance of $K_{pressed}$ below ≈1.5 K. While the turning point of ≈1.5 K may be specific to the strap under investigation, we discuss in the following section that the pressed joints are likely to dominate the sub-Kelvin conductance of such rope straps.

b) Improving the conductance

At practical liquid helium temperatures, the strap conductance can be controlled by altering the braid copper conductivity. For example, the RRR can be raised from 77 to ≈150 following the simple annealing procedure (12 hours at 450^0C in vacuum) by Risegari [**16**], which will improve the K_{strap} by about the same factor. Additionally, K_{strap} at these temperatures can be altered by shortening or lengthening the braid. **Figure 7** shows projected conductance of straps with combinations of RRR 150 and RRR 77, and braid lengths of 100 mm and 150 mm. The graph shows that braid modifications can bring about almost half an order of magnitude improvement at the warmest temperature. As pointed out in the previous section and apparent in **figure 7**, the sub-Kelvin conductance does not change significantly with braid alteration as the conductance here it is dominated by the pressed ends.

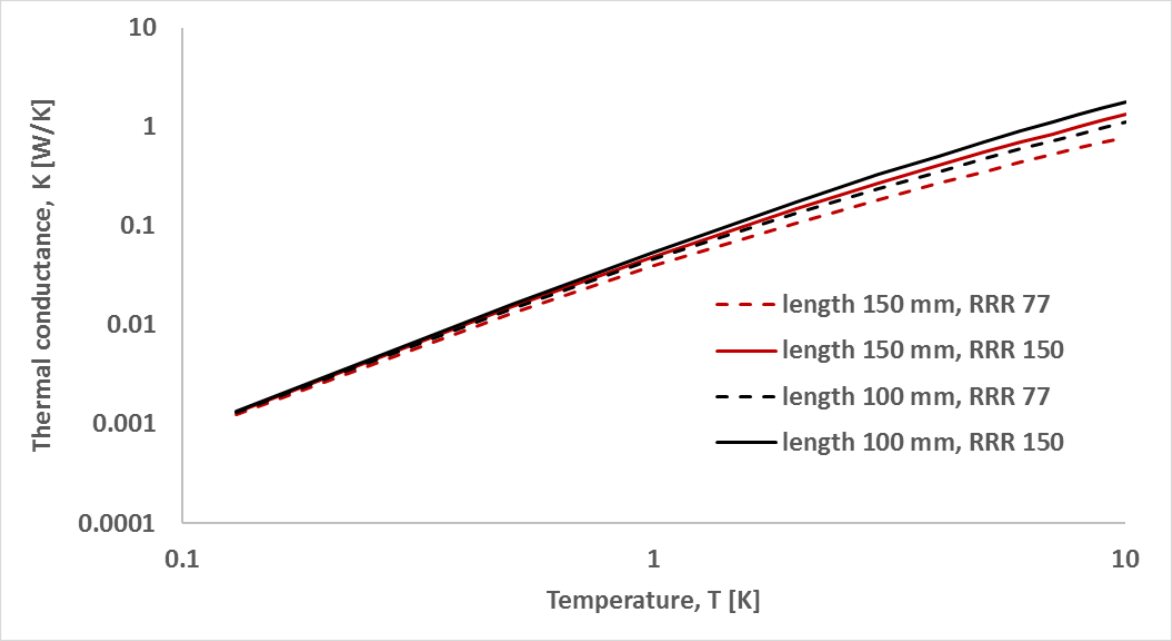

Figure 7: Projected conductance of straps with 1) length 150 mm, RRR 150 (solid red line); 2) length 100 mm, RRR 77 (dashed black line); 3) length 100 mm, 150 RRR (solid black line). Also shown for comparison is the measured conductance of the 150 mm, RRR 77 strap (dashed black line).

At lower temperatures, the pressed conductance can be improved by fusing the ropes to the end-lugs by methods such as electron-beam welding. The fusion will convert the mechanically pressed contact into a solid copper connection and thereby eliminate the phonon contribution to the pressed conductance. Conduction will now be electronic, which varies linearly with temperature. The welding process, although known to be effective in the case of copper foil straps **[5]**, to the best of our knowledge, has not be attempted to fuse strand-woven ropes to solid copper. **Figure 8** shows the result of our developmental work, wherein we obtained a full

penetration electron-beam (e-beam) weld into the end-lugs of the rope strap. **Table 4** lists the e-beam parameters used in the developmental welding. In **figure 9**, we plot and compare the measured conductance of a welded strap (100 mm, RRR 77) to that of its braid. Also included for comparison is the projected conductance of this strap without the welding.

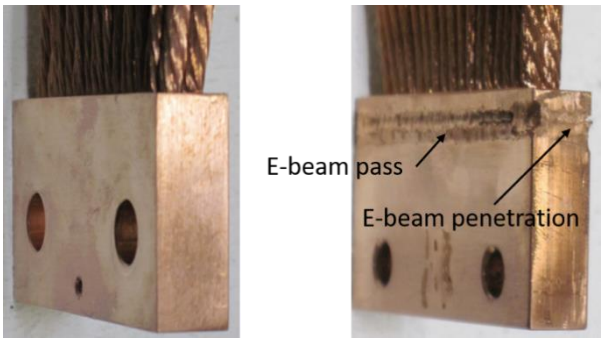

(a) (b)

Figure 8: Strap end-lug (a) as-is (b) after e-beam welding.

Table 4: Parameters chosen for developmental e-beam welding

Parameter	Value
Accelerating voltage	50 kV
Beam current	110 mA
Speed of beam pass	40 inch/min

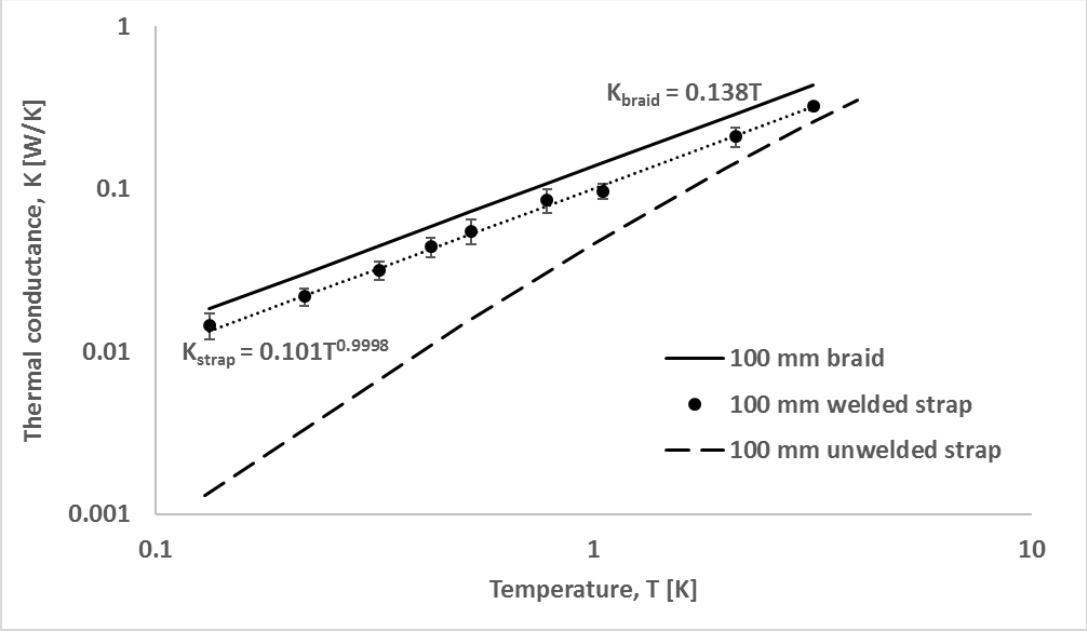

Figure 9: Comparison of braid conductance of a 100 mm, RRR 77 strap (solid line) and the strap conductance (filled circle) after a full penetration electron-beam weld on the end-lugs. Projected conductance of a 100 mm long un-welded strap (dash line) is shown for comparison.

The welded strap shows about an order of magnitude improvement at the lowest temperature with its conductance varying linearly with temperature even below 1.5 K. The magnitude of this conductance approached 70% of that of the braid, which may indicate that not all of the strands were fused with the end-lugs. The welding therefore needs further optimization to attain 100% of the braid conductance and this is a subject of future work.

6. Summary

Thermal conductance of a mechanically-pressed copper rope strap has been measured in the 0.13 K – 10 K temperature range. The conductance varies close to linearly with temperature above ≈1.5 K and nearly as temperature-squared below ≈1.5 K. Pressed contact conductance at the end-lugs dominates the strap conductance at sub-Kelvin temperatures. Electron-beam welding is shown to be a promising technique for improving the sub-Kelvin conductance of the strand-woven copper rope straps but needs optimization to realize the straps' full potential.

7. Acknowledgement

Fermi National Accelerator Laboratory is operated by Fermi Research Alliance, LLC under Contract No. DE-AC02-07CH11359 with the United States Department of Energy. We sincerely thank the SuperCDMS collaboration for supporting this work.

8. References

[1] E. Urquiza, C. Vasques, J. Rodrigues, and B. Van Gorp, Development and testing of an innovative two-arm focal-plane thermal strap (TAFTS), Cryogenics 52, 306-309, 2012. http://dx.doi.org/10.1016/j.cryogenics.2012.01.023

[2] L. Sparr, R. Boyle, L. Nguyen, H. Frisch, S. Banks, E. James, and V. Arillo, Design and test of potential cryocooler cold finger interfaces, Advances in Cryogenic Engineering 39, 1253-1262, 1994. http://dx/doi.org/10.1007/978-1-4615-2522-6_154

[3] K. Kobayahsi and S. Folkman, Stiffness of and vibration transmission through thermal links, AIAA-98-2079, AIAA, 1998. http://dx.doi.org/10.2514/6.1998-2079

[4] S. J. Nieczkoski and E. A. Myers, Highly-conductive graphite thermal straps used in conjunction with vibration isolation mounts for cryocoolers, Cryocoolers 18, 587-597, 2014.

[5] T. Trollier, J. Tanchon, J. Lacapere, P. Renaud, J.C. Rey and A. Ravex, Flexible Thermal Link Assembly Solutions for Space Applications, Cryocoolers 19, 595-603, 2016.

[6] B. Williams, S. Jensen, and J. C. Batty, An advanced solderless flexible thermal link, Cryocoolers 9, 807-812, 1997.

[7] I. Didschuns, A.L. Woodcraft, D. Bintley, and P.C. Hargrave, Thermal conductance measurements of bolted copper to copper joints at sub-Kelvin temperatures, Cryogenics 44, 293–299, 2004. http://dx.doi.org/10.1016/j.cryogenics.2003.11.010

[8] E. Gmelin, M. Asen-Palmer, M. Reuther, and R. Villar, Thermal boundary resistance of mechanical contacts between solids at sub-ambient temperatures. Journal of Physics D-Applied Physics 32(6), 19-43, 1999. https://doi.org/10.1088/0022-3727/32/6/004

[9] A. L. Woodcraft, Comment on 'Thermal boundary resistance of mechanical contacts between solids at sub-ambient temperatures', Journal of Physics D: Applied Physics 34, 2932-2934, 2001. https://doi.org/10.1088/0022-3727/34/18/401

[10] E. Swartz and R. Pohl, Thermal boundary resistance, Review of Modern Physics 61, 605-668, 1989. https://doi.org/10.1103/RevModPhys.61.605

[11] M. J. Nilles, Thermal and electrical contact resistance of OFHC Cu from 4 K to 290 K. Thesis, University of Wisconsin-Madison, 1986.

[12] M.R. Pinnel, H.G. Tompkins, D.E. Heath, Oxidation of copper in controlled clean air and standard laboratory air at 50°C to 150°C, Applications of Surface Science 2(4), 558-577, 1979. http://dx.doi.org/10.1016/0378-5963(79)90047-3

[13] L. J. Salerno, P. Kittel, and A. L. Spivak, Thermal Conductance of Pressed Copper Contacts at Liquid Helium Temperatures, AIAA Journal 22, 1810-1816, 1984. http://dx.doi.org/10.2514/3.8856

[14] R. Berman, Some experiments on thermal contact at low temperatures, Journal of Applied Physics 27(4), 318-323, 1956. http://dx.doi.org/10.1063/1.1722369

[15] NIST cryogenic material properties database, properties of copper available at http://cryogenics.nist.gov/MPropsMAY/OFHC%20Copper/OFHC_Copper_rev1.htm

[16] L. Risegari, M. Barucci, E. Olivieri, E. Pasca, G. Ventura, Measurement of the thermal conductivity of copper samples between 30 and 150 mK, Cryogenics 44, 875-878, 2004. http://dx.doi.org/10.1016/j.cryogenics.2004.01.008